ELSEVIER

Chemical Geology 243 (2007) 275–285

CHEMICAL GEOLOGY
INCLUDING
ISOTOPE GEOSCIENCE

www.elsevier.com/locate/chemgeo

Correlation and comparison of seawater $\delta^{34}S_{sulfate}$ records at the permian-triassic transition

P. Gorjan *, K. Kaiho

Institute of Geology and Paleontology, Tohoku University, Sendai 980–8578 Japan

Received 16 September 2005; received in revised form 4 March 2007; accepted 19 March 2007

Editor: L.M. Walter

Abstract

Correlation of carbonate-associated sulfate (CAS) $\delta^{34}S$-analysed Permian-Triassic (P-Tr) sections via conodont biostratigraphy and sequence stratigraphy shows distinct phases in the oceanic $\delta^{34}S_{sulfate}$ evolution during the period ~1 million years (m.y.) either side of the P-Tr boundary. A $\delta^{34}S_{sulfate}$ rise in the Changhsingian, prior to the end-Permian mass extinction, is followed by a period of about 350,000 years of erratic and substantial $\delta^{34}S_{sulfate}$ movements (range = ~+1‰ to ~+28‰), the mass extinction occurring in the middle of this period. The sharp swings in this phase indicate severe changes in the oceanic sulfur geochemistry, and perhaps stages of ocean inhomogeneity. Low (<+15‰) $\delta^{34}S_{sulfate}$ values coincide with the mass extinction horizon, suggesting the extinction is related to an input of relatively ^{32}S-enriched sulfur into the oceanic sulfate reservoir. The source of this sulfur most likely being H_2S from euxinic waters. After the erratic $\delta^{34}S_{sulfate}$ phase there is a stabilisation of $\delta^{34}S_{sulfate}$ values (~+17‰) until the later Griesbachian. However, there is a possibility of discrepant Panthalassan and Tethyan data sets during the early to mid Griesbachian, but this requires further work for confirmation. $\delta^{34}S_{sulfate}$ values are erratic in the late Griesbachian to early Dienerian, suggesting further perturbation of the sulfur cycle. The poorly age-constrained Smithian record shows a wide range of $\delta^{34}S_{sulfate}$ values probably indicating swings during that time also. The $\delta^{34}S_{sulfate}$ movements from the Changhsingian to Smithian indicate the Permian-Triassic transition is a time of intense changes in the sulfur fluxes to and from the oceans and perhaps stages of ocean inhomogeneity.

Keywords: Permian-Triassic; $\delta^{34}S$; biostratigraphy; CAS; mass extinction; sulfur isotopes

1. Introduction

Several major environmental events coincide at the Permian-Triassic (P-Tr) transition. These include (i) the Phanerozoic's greatest mass extinction; (ii) eruption of the Siberian flood basalts; (iii) severe climate change; (iv) a global cessation in coal production; (v) probable widespread anoxia in the oceans; and (vi) a possible catastrophic bolide impact. Yet despite the intense study of this interval the relationship between these events remains debatable (see reviews by, e.g., Hallam and Wignall, 1997; Erwin et al., 2002; Benton and Twitchett, 2003).

Carbon- and sulfur-isotope geochemical studies can be powerful tools for understanding past environmental changes as reflected in the global carbon and sulfur cycles. But for the P-Tr transition the isotopic record of sulfur has not been so well developed as the carbon-isotope record. The isotopic record of seawater sulfate-sulfur ($\delta^{34}S_{sulfate}$)

* Corresponding author.
E-mail address: psgorjan@yahoo.com (P. Gorjan).

0009-2541/$ - see front matter © 2007 Published by Elsevier B.V.
doi:10.1016/j.chemgeo.2007.03.011

across the P-Tr boundary can record changes in atmospheric, terrestrial, and particularly oceanic conditions, as it monitors the global cycling of sulfur. Thus, this record can offer clues to construct or constrain theories about events at the P-Tr transition. However, an accurate picture of $\delta^{34}S_{sulfate}$ movements is required for this.

Four studies have been published analysing the seawater $\delta^{34}S_{sulfate}$ record across the Permian-Triassic (P-Tr) boundary. Three of these have analysed the carbonate-associated sulfate (CAS; also known as structurally-substituted sulfur, or SSS) of carbonates (Kaiho et al., 2001; Newton et al., 2004; and Korte et al., 2004), while the other (Worden et al., 1997) reports the $\delta^{34}S_{sulfate}$ analysis of evaporite sulfate. However, the results of these studies have, at first appearance, few similarities and to date have not been correlated precisely.

Here we correlate the CAS $\delta^{34}S_{sulfate}$ records of Meishan (South China), Abedah (Iran), and Siusi (Italian Dolomites) sections via conodont biostratigraphy and sequence stratigraphy in order to sift out common patterns in the $\delta^{34}S_{sulfate}$ records and we assign a timescale to these movements based on existing radiometric dates. We also correlate the CAS records with the existing evaporite record (Holser, 1984; Holser et al., 1988) and compare the Panthalassan and Tethyan data (see Fig. 1 for paleolocations of all sections considered in this study). We also discuss possible causes for the movements of the $\delta^{34}S_{sulfate}$ record.

2. Methods

2.1. Correlation of CAS records (Fig. 2)

Interest in the P-Tr boundary and the associated mass extinction has produced a large body of work related to correlating P-Tr sections around the globe. Conodont biostratigraphy has emerged as the most refined correlation tool for this time. Both the Meishan and Abedah P-Tr sections have had conodont zones assigned (Mei et al., 1998; Yin et al., 2001; Korte et al., 2004) allowing a robust correlation. Although no conodont work has been published for the Siusi section it is possible to assign approximate conodont zones by comparison with other sections from the Italian Dolomites that have been analysed (i.e., the Tesero and Bulla sections; Perri, 1991). The comparison involves estimating the boundaries of the conodont zones in relation to the formation boundaries, and then applying it to the Siusi section (see Appendix for details).

Conodonts are not found below the Tesero Oolite Horizon (TOH) of the Italian Dolomites (*Hindeodus latidentatus* is the oldest conodont found). Thus, an alternative means of correlation is required. Here we employ sequence stratigraphy. We correlate the sequence boundary at the base of bed 24e at Meishan with the sequence boundary recognised by Hallam and Wignall (1999) and Newton et al. (2004) about 5 m below the TOH at the Siusi section. This correlation scheme was devised by Wignall and Hallam (1992, 1993), based on the hypothesis of a global regression at this time.

Once correlatable boundaries are assigned to each section (i.e., conodont zone boundaries and sequence stratigraphic boundaries) these are then aligned on a composite column with linear scaling between boundaries. The correlated results are then projected onto a timescale based upon Bowring et al.'s (1998) radiometric dating of ash beds from the Meishan section(s). Details on the construction of Fig. 2 can be seen in Appendix 1.

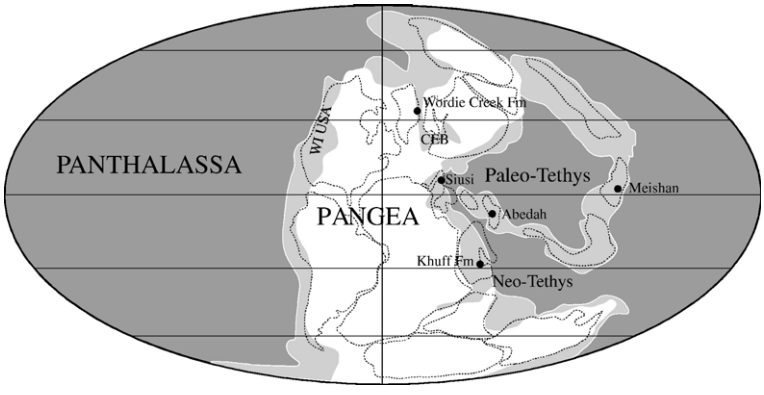

Fig. 1. Paleogeographic map at the P-Tr transition (after Golonka and Ford, 2000), identfiying the paleolocation of all sections considered in this study. WI USA = Western Interior USA. CEB = Central European Basin.

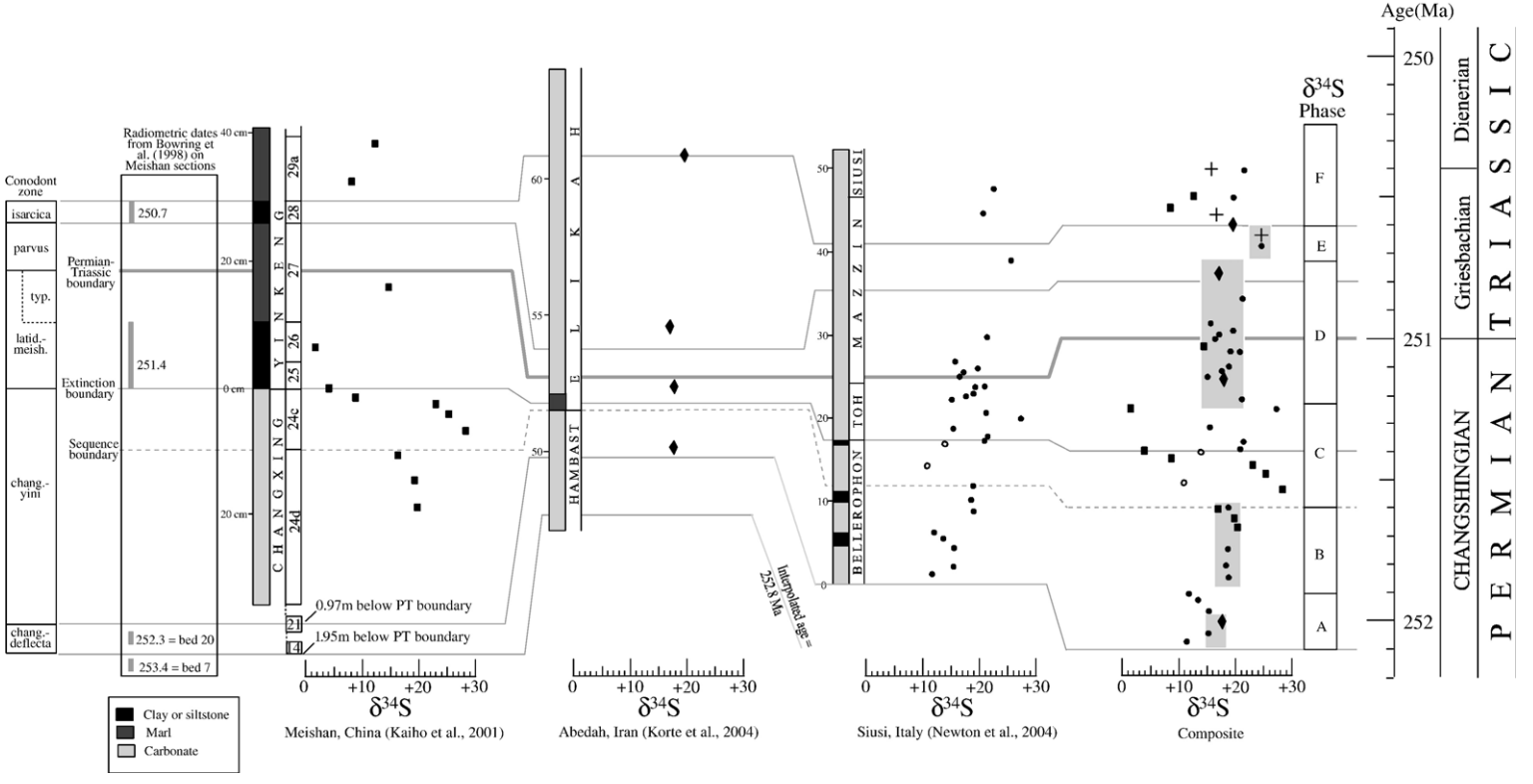

Fig. 2. Correlation of the Meishan, Abedah, and Siusi P-Tr sections via conodont biostratigraphy and sequence stratigraphy, with associated $\delta^{34}S_{sulfate}$ data. Timescale is according to the GTS2004 (Gradstein et al., 2004). Shaded areas on $\delta^{34}S_{sulfate}$ composite plot show interpreted $\delta^{34}S_{sulfate}$ movements, based on points of consistency between $\delta^{34}S_{sulfate}$ of different sections. Column with labels A-F indicate different $\delta^{34}S_{sulfate}$ phases in this time period (see text for details). Thickness of lithological logs are in metres, except for Meishan which is in centimetres. Crosses are from Sosio, analyses and ages by Kampschulte and Strauss (2004). Open circles in Siusi and composite plots are samples showing high $\delta^{18}O_{carb}$ values, possibly indicating diagenesis and thus $\delta^{34}S_{sulfate}$ alteration. TOH = Tesero Oolite Horizon. Conodont zones: isarcica = *Isarcicella isarcica*; parvus = *Hindeodus parvus*; typ. = *Hindeodus Typicalus*; latid.-meish. = *Hindeodus latidentatus-Clarkina meishansensis*; chang.-yini = *Clarkina changxingensis-Clarkina yini*; chang.-deflecta = *Clarkina changxingensis-Clarkina deflecta*.

2.2. Compilation of evaporite data (Table 1; Fig. 3)

Table 1 is a compilation of known Changhsingian to Smithian marine $\delta^{34}S_{sulfate}$ data. This data drawn from Holser (1984) and Holser et al. (1988) compilation, with the exception of newer Zechstein data from Kampschulte et al. (1998). However, we omit data from the Central European Basin (CEB) Buntsandstein deposits (Griesbachian) from Holser et al.'s compilation, as the sulfates therein are probably derived from the underlying Permian salts (Holser and Magaritz, 1987). However, the Changhsingian evaporites of the CEB (Zechstein evaporites) are marine, as testified to by bromine contents of >100 ppm in halite in the Z5 and Z6 horizons (Käding, 2003; suggesting the evaporite is not recycled salt; Holser, 1979); and the extremely low $^{87}Sr/^{86}Sr$ signatures (Kramm and Wedepohl, 1991; Kampschulte et al., 1998), which are amongst the lowest of the Phanerozoic.

A peculiarity of Holser et al.'s evaporite record was that all Griesbachian, Dienerian, and Smithian data came from Boreal and Panthalassan Ocean sites, i.e., western-interior USA (WI USA); and the Central European Basin (CEB), an intra-continental sea covering the present-day Germany, Netherlands, England, Poland, and North Sea.

In this study we have attempted improve the age constraints of the evaporite $\delta^{34}S_{sulfate}$ data from Holser et al.'s assignment to stages. We suggest refinements to the following, (i) Zechstein Z5 data is 252.1 to 252.5 Ma; (ii) the Fiamazza facies of the Bellerophon Formation can be constrained to lower Changhsingian time; (iii) the WI USA data is further constrained, mainly by magnetostratigraphy; and (iv) the Wordie Creek Formation data is lower Griesbachian. These are discussed below.

(i) The youngest Zechstein $\delta^{34}S_{sulfate}$ data comes from the Z5 horizon. $\delta^{34}S_{sulfate}$ data from lower horizons have identical $\delta^{34}S_{sulfate}$ values (Kampschulte et al., 1998), and so are not plotted in this compilation. The Z5 horizon can be correlated to the Meishan section by magnetostratigraphy (Zhu and Liu, 1999; Yin et al., 2001; Szurlies et al., 2003; Nawrocki, 2004). Nawrocki (2004) correlates

Table 1
List of previously published Changhsingian to Smithian evaporite $\delta^{34}S_{sulfate}$ data (excluding Buntsandstein data, or any Zechstein evaporite data below the Z5 cycle; and data of Worden et al., 1997, which is discussed in the text)

Formation, location	Age	$\delta^{34}S$	Reference ($\delta^{34}S$)	Reference (age)
Bellerophon Fm., Fiamazza facies, Southern Alps, Italy	Mid to lower Changhsingian	+9.3 +10.2 +13.8 +12.0 +12.2 +11.7	Cortecci et al., 1981	Cassinis et al., 2002
Zechstein (Z5), Germany	Changhsingian 252.1–252.4 Ma	+11.1 +11.1 +11.4	Kampschulte et al., 1998	Nawrocki, 2004; Szurlies et al., 2003
Wordie Creek Fm., East Greenland	Griesbachian (*G. martini* zone)	+13.5	Clemmensen et al., 1985	Wignall and Twitchett, 2002
Dinwoody Fm., Wyoming, USA	Griesbachian	+9.0 +11.2 +10.3 +10.0 +8.2 +9.4	Wilgus, 1981; Holser et al., 1984, 1988	see Section 2.2
Tenderfoot Mbr., Moenkopi Fm., Utah, USA	Griesbachian-Dienerian	+7.1 +15.6 +17.0	Wilgus, 1981; Holser et al., 1984, 1988	see Section 2.2
Lower Slope-Forming Mbr., Moenkopi Fm., Utah, USA	Griesbachian-Dienerian	+22.0 +23.1	Wilgus, 1981; Holser et al., 1984, 1988	see Section 2.2
Sewemup Mbr. Moenkopi Fm., Utah, USA	Smithian	+12.3 +10.8	Wilgus, 1981; Holser et al., 1984, 1988	see Section 2.2
Lower Red Mbr., Moenkopi Fm., Utah, USA	Smithian-Spathian	+13.6 +9.9 +13.7 +20.2	Wilgus, 1981; Holser et al., 1984, 1988	see Section 2.2
Werfen Fm., Campil Mbr., Val d'Adige, Italy	Smithian	+26.5 +27.1 +26.9	Cortecci et al., 1981	Twitchett, 1999

Z5 with Meishan bed 21, i.e, ~1.1 m.y. prior to the P-Tr boundary (from the timescale in Fig. 2). If a more traditional magnetostratigraphic correlation is used (e.g., Szurlies et al., 2003) then Z5 would correlate with Meishan beds 17–19, which are ~1.5 m.y. prior to the P-Tr boundary (from the timescale in Fig. 2). Thus we assign this $\delta^{34}S_{sulfate}$ data an age of 252.1 to 252.5 Ma on Fig. 3.

(ii) The Fiamazza facies is the evaporitic facies of the Bellerophon Formation (Italian Dolomites) that lies below the upper carbonates. In the Siusi section of Fig. 1 it lies below the section drawn, and thus is older than 252.1 Ma. However, Cassinis et al. (2002) constrain the Bellerophon Formation to a Changhsingian age. Thus, the oldest possible age for this data is the base of the Changhsingian, which is 254 Ma on Fig. 3. Thus, this $\delta^{34}S_{sulfate}$ data set is set an age of 252.2 to 254 Ma on Fig. 3.

(iii) The Dinwoody Formation $\delta^{34}S_{sulfate}$ samples (see Table 1) come from central Wyoming, USA. The Dinwoody Formation in Wyoming is the result of a rapid earliest Triassic transgression across the gently sloping Wyoming shelf, from west to east (Collinson and Hasenmueller, 1978; Carr and Paull, 1983). The basal Dinwoody Formation is early Griesbachian, preserving the conodont *Hindeodus parvus* in western Wyoming, with the more eastward Dinwoody Formation probably being too hypersaline for conodont fauna (Paull and Paull, 1994). In Wyoming the Dinwoody Formation grades vertically and laterally into the continental red beds of the

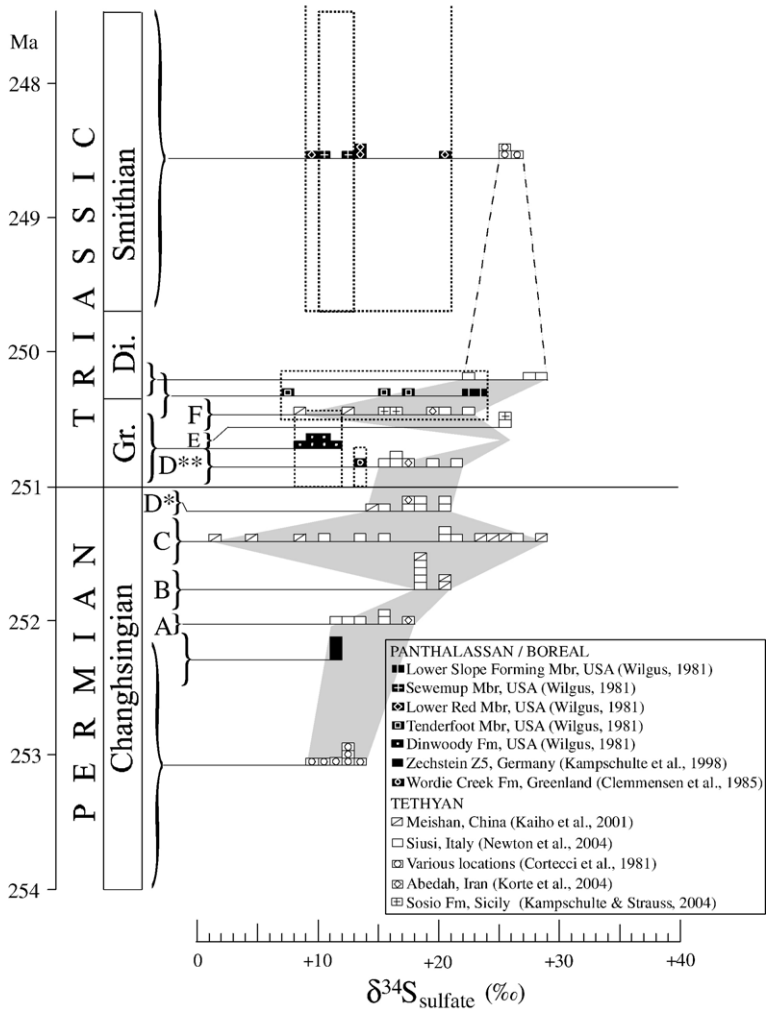

Fig. 3. Histograms of $\delta^{34}S_{sulfate}$ data compiled for the Griesbachian (Gr.), Dienerian (Di.), and Smithian. Changhsingian $\delta^{34}S_{sulfate}$ data from Kampschulte et al. (1998) is representative of all Zechstein values (i.e., average ~ +11‰) (see Section 2.2 for discussion on age assignments). Labels A-F are $\delta^{34}S_{sulfate}$ phases from Fig. 2, with D* and D** being only the Changhsingian and Griesbachian parts of phase D, respectively. Shaded area connects the Tethyan CAS data. Dashed-line rectangles represent limits of evaporitic (Panthalassan) $\delta^{34}S_{sulfate}$. Timescale according to the GTS2004 (Gradstein et al., 2004).

Red Peak Formation (Chugwater Group). The Red Peak Formation began prograding westward across the Wyoming shelf in the late Griesbachian and continuing throughout the Dienerian, stopping at the edge of the deepwater paleo-basin in southeastern Idaho (Carr and Paull, 1983). This means that the top of the Dinwoody Formation in central Wyoming would be within the Griesbachian. This is consistent with magnetostratigraphic results. Shive et al. (1984) and Picard (1964) show three short normal (unreversed) intervals in the Red Peak Formation of Wyoming. Regional and international magnetostratigraphic correlation put the oldest of these intervals near the Griesbachian-Dienerian boundary (Haag and Heller, 1991; Ogg and Steiner, 2001; Molina Garza et al., 2000; Gallet et al., 2000). Furthermore, this lowest normal interval is more than 100 m above the Dinwoody-Red Peak contact. We therefore assign an age of basal to late Griesbachian for the Dinwoody Formation $\delta^{34}S_{sulfate}$ values in Fig. 3.

Steiner et al. (1993) suggest an upper Griesbachian to lower Dienerian age for the Tenderfoot and Hoskininni Members (Moenkopi Formation), based on magnetostratigraphy. The Lower Slope Forming Member (of the Moenkopi Formation) is also approximately coeval with the Hoskininni Member (Blakey, 1974; Shoemaker and Newman, 1959). We therefore place these $\delta^{34}S_{sulfate}$ data in the upper Griesbachian to lower Dienerian in Fig. 3.

Magnetostratigraphic evidence for the Sewemup Member of the Moenkopi Formation (Helsley and Steiner, 1974) suggests a Smithian age by comparison with international magnetostratigraphic composites (Haag and Heller, 1991; Ogg and Steiner, 2001).

The Lower Red Member of the Moenkopi Formation overlies the basal Smithian *Meekoceras*-bearing beds of the Timpoweap Member (Lucas et al., 2004), and is overlain by the Spathian *Tirolites*-bearing Virgin Limestone Member (Stewart et al., 1972). Thus, the Lower Red Member is Smithian to Spathian in age.

(iv) The Wordie Creek Formation $\delta^{34}S_{sulfate}$ data comes from the *Glyptophiceras martini* ammonoid zone which is early Griesbachian (Wignall and Twitchett, 2002), and plotted in the lower half of the Griesbachian in Fig. 3.

In order to compare the CAS data with the evaporite data we present in Fig. 3 the CAS data (Kaiho et al., 2001; Newton et al., 2004; and Korte et al., 2004; from Fig. 2) in histogram form. Histograms of the CAS data are constructed by grouping the data according to their phase, as presented in Fig. 2. In contrast to Holser's (1984) and Holser et al.'s (1988) compilation all of the CAS data is Tethyan in origin.

Internationally correlatable boundaries are difficult to assign in the latest Permian Khuff Formation of United Arab Emirates (Stephenson et al., 2003) and so the evaporite $\delta^{34}S_{sulfate}$ data of Worden et al. (1997) is not plotted in Fig. 3.

3. Results

3.1. Correlation of CAS records (Fig. 2)

The results of this correlation are shown in Fig. 2. Although the $\delta^{34}S_{sulfate}$ patterns still show some discrepancies this correlation scheme has shown several points of contact between them. We observe six different phases in the $\delta^{34}S_{sulfate}$ record (labeled A-F on Fig. 2). (The variation in $\delta^{34}S_{sulfate}$ may well be due to diagenesis (Kampschulte and Strauss, 2004), but this process is poorly understood. However, a significant observation comes from the Zechstein evaporites, which show $\delta^{34}S_{sulfate}$ to have a 5‰ range, but consistently average ~+11‰. This suggests changes of 2–3‰, positive and negative, can be expected with $\delta^{34}S_{sulfate}$ data.)

Phase A: This phase shows a $\delta^{34}S_{sulfate}$ between ~+10‰ and ~+16‰. The high values of Siusi approximate the Abedah section datum.

Phase B: There is a consistent value of ~+19‰ at two locations (Siusi and Meishan) just prior to the sequence boundary.

Phase C: This interval shows the greatest variation in $\delta^{34}S_{sulfate}$. The highest values at both Siusi and Meishan are recorded in this short interval (Abedah data is missing in this interval). Low values occur at the extinction level. However, the high values cannot be correlated as they lie on either side of the extinction level, as noted by Newton et al. (2004). Also, an exact relationship between $\delta^{34}S_{sulfate}$ and the extinction level is not robustly established here due to uncertainty of the precise extinction level at Siusi. According to the timescale of Fig. 2 this period of volatility lasted ~350,000 years.

Phase D: There is a levelling out of $\delta^{34}S_{sulfate}$ in the *Hindeodus latidentatus-Clarkina meishansensis* zone, and continues into the *Hindeodus parvus* zone. Three sections (Meishan, Abedah, and Siusi) show values averaging ~+17‰ with a range of + or -3‰. This steady phase D continues until the *Isarcicella isarcica* zone, a period of about 500,000 years.

Phase E: $\delta^{34}S_{sulfate}$ rises to a high of ~+25‰ in the *Isarcicella isarcica* zone. This high is established at two sections, Siusi and Sosio (Sicily; data from Kampschulte and Strauss, 2004). This spike is short-lived, less than 200,000 years.

Phase F: $\delta^{34}S_{sulfate}$ values plunge at the top of the *Isarcicella isarcica* zone to ~+16‰ (average). This phase shows a large amount of scatter. Values at Meishan

are lower than average and those at Siusi are slightly higher than average. Alternatively, it is possible that there is a drop to <+10‰ after the *Isarcicella Isarcica* zone before rising again.

3.2. Comparison of the evaporite (Panthalassan) and CAS (Tethyan) $\delta^{34}S_{sulfate}$ records (Fig. 3)

As the Tethyan $\delta^{34}S_{sulfate}$ data is reasonably continuous from the late Changhsingian to the end-Griesbachian, it provides a template for comparison with the Panthalassan data for this time. However, the stratigraphic uncertainty of the evaporite data makes comparison difficult. The Panthalassan Zechstein Z5 data correlates well with the Tethyan data. But there is potential for discrepancy in the early to mid Griesbachian, where Tethyan data is a minimum of 15‰, but the weighting of the Panthalassan data is toward lower values (~+10‰), and the single Boreal datum being ~+13‰. The later Griesbachian and early Dienerian sees a significant range (~15‰) in both Panthalassan and Tethyan data sets.

Although it appears as though there is deviation between the Panthalassan and Tethyan $\delta^{34}S_{sulfate}$ records in the Smithian, the data are too few and too poorly age-constrained for both data sets to make a meaningful comparison.

As a whole, the P-Tr transition $\delta^{34}S_{sulfate}$ data shows a tendency to be extremely volatile, certainly in the Tethyan record (note wide range in values, even over short time intervals) and possibly equally so in the Panthalassan, which also shows a significant range in the upper Griesbachian (~15‰).

4. Discussion

This discussion follows the evolution of the seawater $\delta^{34}S_{sulfate}$ signal from the Changhsingian to the Smithian. It is broken up into the following Sections: (4.1) Changhsingian rise in $\delta^{34}S^{sulfate}$; (4.2) $\delta^{34}S_{sulfate}$ volatility associated with the mass extinction (phase C); (4.3) Stabilisation of $\delta^{34}S_{sulfate}$ across the P-Tr boundary and later swings (post-extinction to Dienerian); (4.4) Uncertainty of the Smithian $\delta^{34}S_{sulfate}$ record; and (4.5) Panthalassan versus Tethyan $\delta^{34}S_{sulfate}$ records.

4.1. Changhsingian rise in $\delta^{34}S_{sulfate}$

$\delta^{34}S_{sulfate}$ for the late Permian is well established at ~+11‰ (Claypool et al., 1980), represented in Fig. 3 by the Zechstein (Z5 cycle) and Bellerophon Formation evaporite data. However, at some point before the extinction there is a rise to ~+19‰ (phase B) within the Changhsingian. From Figs. 2 and 3 the beginning of this rise is in the mid-Changhsingian, rising to ~+19‰ within 1 m.y., an extremely rapid rise. (It should be noted that there is some evidence for a slower $\delta^{34}S_{sulfate}$ rise. Evaporite $\delta^{34}S_{sulfate}$ from the Khuff Formation (Worden et al., 1997) suggests a gradual rise, beginning in the first half of the Changhsingian, Also, Korte et al. (2004) record a $\delta^{34}S_{sulfate}$ value of +14.4‰ in the *Clarkina leveni* conodont zone (mid-Wuchiapingian; Mei and Henderson, 2001), suggesting that the rise in $\delta^{34}S_{sulfate}$ may have begun before the Changhsingian.)

Responsibility for the Changhsingian $\delta^{34}S_{sulfate}$ rise can most likely be attributed to a build up of euxinic conditions in the global oceans (a conclusion reached by Newton et al., 2004). Such conditions would see the deposition of ^{32}S-enriched sedimentary sulfide, leaving ^{34}S-enriched sulfide. Evidence for late Permian euxinia is found in numerous places, e.g., Greenland's Ravnefjeld Formation (Nielsen and Shen, 2004), China's Meishan site and western Australia's Perth Basin (Grice et al., 2005), Japan's Panthalassan pelagic terrains (Kajiwara et al., 1994), and the Ursula Creek Section, Canada (Wignall and Newton, 2003). However, why the rise should be so rapid is uncertain, given that the above sections show euxinicity well before the mid-Changhsingian.

4.2. $\delta^{34}S_{sulfate}$ volatility associated with the mass extinction (phase C)

Phase C shows erratic and substantial $\delta^{34}S_{sulfate}$ movements, lasting about 350,000 years. At the middle of this phase lies the mass extinction horizon. The erratic nature of the composite $\delta^{34}S_{sulfate}$ (Fig. 2) in this phase is due, in part, to the differing trends at Meishan and Siusi. At Meishan values go from high to low, while it is opposite at Siusi. Thus, the high values (>+25‰) are below the extinction horizon at Meishan and above at Siusi. This may 'result from proximity to local sulfur sources or other regional changes caused by sporadic basin isolation' (quote from Newton et al., 2004). We add here the possibility that oceanic mixing was severely reduced, or perhaps that different depths had different $\delta^{34}S_{sulfate}$ values (consistent with widespread euxinia). As the beginning of this phase coincides with a transgression (sedimentation resumes after a brief hiatus suggested to be a global sea level fall by Wignall and Hallam (1992, 1993) and Wignall et al. (1996)), it may indicate that the new oceanic geochemical conditions are related to a sea level rise.

At the extinction horizon $\delta^{34}S_{sulfate}$ tends to lower values. Two hypotheses have been proposed to explain the decline in $\delta^{34}S_{sulfate}$. One is an injection of mantle sulfur ($\delta^{34}S$ ~0‰), derived either from volcanism (e.g.,

Koeberl et al., 2002) or extraterrestrial impact (e.g., Kaiho et al., 2001). Another is an upwelling of deep euxinic waters ($\delta^{34}S < 0‰$) that mixed with shallower oxic waters (e.g., Wignall et al., 1996; Newton et al., 2004), which is also the mechanism of extinction.

Given that the concentration of sulfate in late Permian seawater is believed to have been about 0.6 to 0.8 of modern seawater (Kovalevych et al., 2002; Horita et al., 2002; Lowenstein et al., 2005), it would make the late Permian oceans a significant reservoir of sulfur that cannot (in its entirety) be easily perturbed (the residence time of modern oceanic sulfate is in the order of 10 m.y. (Nriagu et al., 1991)). The direct input of volcanically-produced sulfur from the Siberian Traps (Kamo et al., 2003) is insufficient in quantity (less than 1% of the late Permian oceanic reservoir) to produce any significant isotopic change (see calculations by Newton et al., 2004). As Newton et al. (2004) have discussed, intense BSR, producing euxinic waters, and reoxidation of these is a plausible mechanism (quantitatively) for explaining the $\delta^{34}S_{sulfate}$ shifts, as a bacterial reduction of 30% of the total oceanic sulfate reservoir can produce a 15‰ shift in $\delta^{34}S_{sulfate}$. It is possible that the massive volcanic activity of the Siberian Traps helped cause this scenario via the creation of atmospheric pollutants (sulfur and carbon gases, and particles) that inhibit photosynthesis and alter the climate, creating states of hot (via greenhouse gases) and cold (via masking of sunlight). These changes in temperature could translate to changes in water circulation patterns as well as changes in the bacterial sulfate reduction (BSR) quantities and rates.

4.3. Stabilisation of $\delta^{34}S_{sulfate}$ across the P-Tr boundary and later swings (phase D-Dienerian)

Above the extinction level toward the top of the *Hindeodus latidentatus – Clarkina meishansensis* and into the early *Hindeodus parvus* zone there is a consistency in all three CAS studies, $\delta^{34}S_{sulfate}$ being around +17‰. This is also the value recorded in the Khuff Formation evaporites across the P-Tr boundary (Worden et al., 1997). Perhaps this is recording a stabilisation and homogenisation of the oceanic $\delta^{34}S_{sulfate}$ composition after a tumultuous period associated with the extinction. However, we note there is the possibility of deviation between Panthalassan and Tethyan records in the early to mid Griesbachian (see Section 4.5). This phase lasts about 400,000 years. In the later *Isarcicella Isarcica* zone (phase E) there is a rise seen in two sections (Sosio and Siusi). At the top of the *Isarcicella Isarcica* zone values drop again. Phase F appears to have scattered values, but it is uncertain if these follow a particular trend or represent conditions as seen in phase C. Only further detailed work on more sections can resolve this. Nonetheless, the continuation of $\delta^{34}S_{sulfate}$ swings in the Griesbachian and Dienerian shows that oceanic sulfate was still subject to periods of intense alteration from an oceanic mixing/stagnation combination or drastic changes in the fluxes of sulfur to the oceans.

4.4. Uncertainty of the Smithian $\delta^{34}S_{sulfate}$ record

The compilation of Smithian $\delta^{34}S_{sulfate}$ data (Fig. 4) shows a wide range (~20‰). Like the preceding record it indicates that there were swings in $\delta^{34}S_{sulfate}$, but the timing of these swings cannot be evaluated without better constraint on the ages of the $\delta^{34}S_{sulfate}$ values. This also highlights the value in using well-dated sections and fully reporting $\delta^{34}S_{sulfate}$ results against section logs. We note that the erratic nature of the $\delta^{34}S_{sulfate}$ record from the Griesbachian to the Smithian is also a feature of the carbon-isotope record for the early Triassic (Griesbachian to Spathian; Payne et al., 2004), although it is beyond the scope of this study to examine correlations between these.

4.5. Panthalassan versus Tethyan $\delta^{34}S_{sulfate}$ records

As mentioned previously, a possible discrepancy between Panthalassan and Tethyan $\delta^{34}S_{sulfate}$ records is seen in the early to mid Griesbachian (Fig. 3). This can only be stated as a possibility as the stratigraphic position of sampling within the Dinwoody Formation (Table 1) is not stated. More data needs to be collected in order to be certain if these are discrepant records. In particular, it would be crucial to our understanding of the mass extinction to see if there are $\delta^{34}S_{sulfate}$ movements at the extinction level in the Panthalassan realm. However, if there is a difference in $\delta^{34}S_{sulfate}$ between Panthalassan and Tethyan waters, the cause of this could conceivably be land bridges on the eastern Tethys (see Fig. 1) combined with a sluggish ocean. Modelling of P-Tr oceanic circulation by Kiehl and Shields (2005) suggests the possibility of this.

5. Conclusion

Correlation and comparison of the existing $\delta^{34}S_{sulfate}$ record across the P-Tr transition shows a complex history, which probably reflects the complexity of environmental events in this interval. This may also indicate that pursuit of detailed $\delta^{34}S_{sulfate}$ studies will be a fruitful area of research for understanding the environmental events and oceanic conditions of the P-Tr transition.

We have identified a rapid rise in $\delta^{34}S_{sulfate}$ during the Changhsingian, probably due a period of intense

BSR. This was followed by a period of volatile $\delta^{34}S_{sulfate}$ movement, that may suggest ocean inhomogeneity. The end-Permian mass extinction lies within this phase. At the extinction horizon $\delta^{34}S_{sulfate}$ tends to low values that indicates an injection of ^{32}S-enriched sulfur to the oceanic sulfate reservoir, probably from the oxidation of H_2S in euxinic waters.

From the late Griebachian to the Smithian there are continued shifts in $\delta^{34}S_{sulfate}$, suggesting that environmental conditions had not stabilised in the early Triassic. The possibility of discrepant $\delta^{34}S_{sulfate}$ records in the Panthalassan versus the Tethyan requires further data to be confirmed.

Acknowledgements

The authors thank the Japan Society for the Promotion of Science (JSPS) for the financial support required for this study. We also thank J.K. Nielsen and an anonymous reviewer for critical comments that greatly improved this study.

Appendix: Construction of Fig. 2

Correlation of Isarcicella Isarcica zone:

The *Isarcicella Isarcica* zone was directly determined for Abedah (Korte et al., 2004) and Meishan (Yin et al., 2001). No conodont work has been published for Siusi, thus comparison to other Italian Dolomite sections is used to estimate conodont levels. Conodont work has been published for the Bulla and Tesero sections (Perri, 1991; also Perri and Andraghetti, 1987, their Fig. 5). The Bulla section is used as it is closer to the Siusi section (but note that little difference would result if the Tesero section is used). At Bulla the *Isarcicella isarcica* zone begins about half-way up the Mazzin Member and ends at about three-quarters up. (At Tesero the isarcica zone begins about a third of the way up and ends about 85% of the way up.) Thus, at Siusi it is placed from half-way to three-quarters up in the Mazzin Member.

Above the Isarcicella isarcica zone:

Scaling above the *Isarcicella isarcica* zone is maintained as in the *Isarcicella isarcica* zone (i.e., sedimentation rate is assumed constant).

Correlation of sequence boundary:

The sequence boundary is used to correlate the Siusi and Meishan sections, as no conodonts extend below the *Hindeodus latidentatus* zone in the Italian Dolomites. A global regression is suggested by Wignall and Hallam (1992, 1993; also Yin and Tong, 1998) just prior to the extinction boundary. This level was determined for Meishan (Yin et al., 2001) and Siusi (Hallam and Wignall, 1999; Newton et al., 2004). The Abedah section has erosional surface at the *Clarkina hauschkei* zone, and this is assumed to be the same level, but this correlation is unimportant for Abedah as no $\delta^{34}S_{sulfate}$ points fall in this level.

Correlation of Clarkina changxingensis-yini and Clarkina changxingensis-deflecta zones:

Determined for Meishan (Mei et al., 1998) and Abedah (Korte et al., 2004). Lack of late Permian conodont data from the Italian Dolomites means correlation for Siusi not possibe via this method. In this case no correlation is done, the $\delta^{34}S_{sulfate}$ data is simply scaled (against the timescale) as it was for data between the sequence boundary and the base of the *Hindeodus latidentatus* zone.

Also, the hiatus caused the proposed by global regression creating a depositional hiatus is suggested be longer at the Italian Dolomites than at Meishan (Wignall and Hallam, 1992, 1993) therefore the Siusi data is placed below the Meishan data on the composite $\delta^{34}S_{sulfate}$ curve.

The *Clarkina changxingensis-yini* zone correlates with the *Clarkina hauschkei* zones (Korte et al., 2004) as *Clarkina hauschkei* is found in top 6 cm of bed 24 at Meishan.

References

Benton, M.J., Twitchett, R.J., 2003. How to kill (almost) all life: the end-Permian extinction event. Trends in Ecology and Evolution 18, 358–365.

Blakey, R.C., 1974. Stratigraphic and depositional analysis of the Moenkopi Formation, southeastern Utah. Utah Geological and Mineral Survey Bulletin 104, 45–76.

Bowring, S.A., Erwin, D.H., Jin, Y.G., Martin, M.W., Davidek, K.L., Wang, W., 1998. U/Pb zircon geochronology and tempo of the end-Permian mass extinction. Science 291, 1530–1533.

Carr, T.R., Paull, R.K., 1983. Early Triassic stratigraphy and paleogeography of the Cordilleran miogeosyncline. In: Reynolds, M.W., Dolly, E.D. (Eds.), Mesozoic Paleogeography of the West-Central United States. SEPM, Denver, pp. 39–55.

Cassinis, G., Nicosia, U., Lozovsky, V.R., Gubin, Y.M., 2002. A view on the Permian continental stratigraphy of the Southern Alps, Italy, and general correlation with the Permian of Russia. Permophiles 40, 4–16.

Claypool, G.E., Holser, W.T., Kaplan, I.R., Sakai, H., Zak, I., 1980. The age curves of sulfur and oxygen isotopes in marine sulfate and their mutual interpretation. Chemical Geology 28, 199–260.

Clemmensen, L., Holser, W.T., Winter, D., 1985. Stable isotope study through the Permian-Triassic boundary in East Greenland. Bulletin of the Geological Society of Denmark 33, 253–260.

Collinson, J.W., Hasenmueller, W.A., 1978. Early Triassic paleogeography and biostratigraphy of the Cordilleran miogeosyncline. In: Howell, D.G., McDougall, K.A. (Eds.), Mesozoic Paleogeography of the Western United States. SEPM, pp. 175–187.

Cortecci, G., Reyes, E., Berti, G., Casati, P., 1981. Sulfur and oxygen isotopes in Italian marine sulfates of Permian and Triassic ages. Chemical Geology 34, 65–79.

Erwin, D.H., Bowring, S.A., Jin, Y., 2002. End-Permian mass extinctions: A review In: Koeberl, C., MacLeod, K.G. (Eds.), Catastrophic Events and Mass Extinctions: Impacts and Beyond. Geological Society of America, Boulder, pp. 363–383.

Gallet, Y., Krystyn, L., Besse, J., Saidi, A., 2000. New constraints on the Upper Permian and Lower Triassic geomagnetic polarity timescale from the Abadeh section (central Iran). Journal of Geophysical Research 105 (B2), 2805–2815.

Golonka, J., Ford, D., 2000. Pangean (Late Carboniferous–Middle Jurassic) paleoenvironment and lithofacies. Palaeogeography, Palaeoclimatology, Palaeoecology 161, 1–34.

Gradstein, F.M., Ogg, J.G., Smith, A.G., Agterberg, F.P., Bleeker, W., Cooper, R.A., Davydov, V., Gibbard, P., Hinnov, L.A., House, M.R., Lourens, L., Luterbacher, H.P., McArthur, J., Melchin, M.J., Robb, L.J., Shergold, J., Villeneuve, M., Wardlaw, B.R., Ali, J., Brinkhuis, H., Hilgen, F.J., Hooker, J., Howarth, R.J., Knoll, A.H., Laskar, J., Monechi, S., Plumb, K.A., Powell, J., Raffi, I., Röhl, U., Sadler, P., Sanfilippo, A., Schmitz, B., Shackleton, N.J., Shields, G.A., Strauss, H., Van Dam, J., van Kolfschoten, T., Veizer, J., Wilson, D., 2004. A Geologic Time Scale 2004. Cambridge University Press, Cambridge.

Grice, K., Cao, C., Love, G.D., Bottcher, M.E., Twitchett, R.J., Grosjean, E., Summons, R.E., Turgeon, S.C., Dunning, W., Jin, Y., 2005. Photic-zone euxinia during the Permian-Triassic superanoxic event. Science 307, 706–709.

Haag, M., Heller, F., 1991. Late Permian to Early Triassic magnetostratigraphy. Earth and Planetary Science Letters 107, 42–54.

Hallam, A., Wignall, P.B., 1997. Mass Extinctions and their Aftermath. Oxford University Press, Oxford.

Hallam, A., Wignall, P.B., 1999. Mass extinctions and sea level changes. Earth-Science Reviews 48, 217–250.

Helsley, C.E., Steiner, M.B., 1974. Paleomagnetism of the Lower Triassic Moenkopi Formation. Geological Society of America Bulletin 85, 457–464.

Holser, W.T., 1979. Trace elements and isotopes in evaporites. In: Burns, R.G. (Ed.), Marine Minerals, Reviews in Mineralogy, 6–21. Mineralogical Society of America, Washington, pp. 295–346.

Holser, W.T., 1984. Gradual and abrupt shifts in ocean chemistry during Pha nerozoic time. In: Holland, H.D., Trendall, A.F. (Eds.), Patterns of Change in Earth Evolution. Springer-Verlag, Berlin, pp. 123–143.

Holser, W.T., Magaritz, M., 1987. Events near the Permian-Triassic boundary. Marine Geology 11, 155–180.

Holser, W.T., Schidlowski, M., MacKenzie, F.T., Maynard, J.B., 1988. Geochemical cycles of carbon and sulfur In: Gregor, C.B., Garrels, R.M., MacKenzie, F.T., Maynard, J.B. (Eds.), Chemical Cycles in the Evolution of the Earth. Wiley, New York, pp. 105–173.

Horita, J., Zimmermann, H., Holland, H.D., 2002. Chemical evolution of seawater during the Phanerozoic: Implications from the record of marine evaporites. Geochimica et Cosmochimica Acta 66, 3733–3756.

Käding, K.C., 2003. Bromprofile aus dem Zechstein 4 und 5 – ein Beitrag zur Stratigraphie der Aller- und Ohre-Folge. Kali und Steinsalz 1/2003, 6–17.

Kaiho, K., Kajiwara, Y., Nakano, T., Miura, Y., Kawahata, H., Tazaki, K., Ueshima, M., Chen, Z., Shi, G.R., 2001. End Permian catastrophe by a bolide impact: evidence of a gigantic release of sulfur from the mantle. Geology 29, 815–818.

Kajiwara, Y., Yamakita, S., Ishida, K., Ishiga, H., Imai, A., 1994. Development of a largely anoxic stratified ocean and its temporary massive mixing at the Permian/Triassic boundary supported by the sulfur isotopic record. Palaeogeography, Palaeoclimatology, Palaeoecology 111, 367–379.

Kamo, S.L., Czamanske, G.K., Amelin, Y., Fedorenko, V.A., Davis, D.W., Trofimov, V.R., 2003. Rapid eruption of Siberian flood-volcanic rocks and evidence for coincidence with the Permian-Triassic boundary and mass extinction at 251 Ma. Earth and Planetary Science Letters 214, 75–91.

Kampschulte, A., Strauss, H., 2004. The sulfur isotopic evolution of Phanerozoic seawater based on the analysis of structurally substituted sulfate in carbonates. Chemical Geology 204, 255–286.

Kampschulte, A., Buhl, D., Strauss, H., 1998. The sulfur and strontium isotopic compositions of Permian evaporites from the Zechstein basin, northern Germany. Geologische Rundschau 87, 192–199.

Kiehl, J.T., Shields, C.A., 2005. Climate simulation of the latest Permian: implications for mass extinction. Geology 33, 757–760.

Koeberl, C., Gilmour, I., Reimold, W.U., Claeys, P., Ivanov, B.A., 2002. End-Permian catastrophe by bolide impact: Evidence of a gigantic release of sulfur from the mantle: Comment. Geology 30, 855–856.

Korte, C., Kozur, H.W., Joachimski, M.M., Strauss, H., Veizer, J., Schwark, L., 2004. Carbon, sulfur, oxygen and strontium isotope records,organic geochemistry and biostratigraphy across the Permian/Triassic boundary in Abadeh, Iran. International Journal of Earth Sciences 93, 565–581.

Kovalevych, V.M., Peryt, T.M., Carmona, V., Sydor, D.V., Vovnyuk, S.V., Halas, S., 2002. Evolution of Permian seawater: evidence from fluid inclusions in halite. Neues Jahrbuch fur Mineralogie. Abhandlungen 178, 27–62.

Kramm, U., Wedepohl, K.H., 1991. The isotopic composition of strontium and sulfur in seawater of Late Permian (Zechstein) age. Chemical Geology 90, 253–262.

Lowenstein, T.K., Timofeeff, M.N., Kovalevych, V.M., Horita, J., 2005. The major-ion composition of Permian seawater. Geochimica et Cosmochimica Acta 69, 1701–1719.

Lucas, S.G., Milner, A.R.C., Vice, G.S., 2004. Early Triassic (Smithian) paleogeography and ammonites in southwestern Utah. Geological Society of America Abstracts with Programs 36, 363.

Mei, S., Henderson, C.M., 2001. Evolution of Permian conodont provincialism and its significance in global correlation and paleoclimate implications. Palaeogeography, Palaeoclimatology, Palaeoecology 170, 237–260.

Mei, S., Zhang, K., Wardlaw, B.R., 1998. A refined succession of Changhsingian and Griesbachian neogondolellid conodonts from the Meishan section, candidate of the global stratotype section and point of the Permian–Triassic boundary. Palaeogeography, Palaeoclimatology, Palaeoecology 143, 213–226.

Molina Garza, R.S., Geissman, J.W., Lucas, S.G., 2000. Palaeomagnetism and magnetostratigraphy of uppermost Permian strata, southeast New Mexico, USA: correlation of the Permian–Triassic

boundary in non-marine environments. Geophysical Journal International 141, 778–786.

Nawrocki, J., 2004. The Permian–Triassic boundary in the Central European Basin: magnetostratigraphic constraints. Terra Nova 16, 139–145.

Newton, R.J., Pevitt, E.L., Wignall, P.B., Bottrell, S.H., 2004. Large shifts in the isotopic composition of seawater sulphate across the Permo-Triassic boundary in northern Italy. Earth and Planetary Science Letters 218, 331–345.

Nielsen, J.K., Shen, Y., 2004. Evidence for sulfidic deep water during the Late Permian in the East Greenland Basin. Geology 32, 1037–1040.

Nriagu, J.O., Rees, C.E., Mekhtiyeva, V.L., Yu Lein, A., Fritz, P., Drimmie, R.J., Pankina, R.G., Robinson, B.W., Krouse, H.R., 1991. Hydrosphere. In: Krouse, H.R., Grinenko, V.A. (Eds.), Stable Isotopes: Natural and Anthropogenic Sulfur in the Environment. John Wiley and Sons, Chichester, pp. 177–266.

Ogg, J.G., Steiner, M.B., 2001. Early Triassic polarity time-scale—integration of magnetostratigraphy, ammonite zonation and sequence stratigraphy from stratotype sections (Canadian Arctic Archipelago). Earth and Planetary Science Letters 107, 69–89.

Paull, R.K., Paull, R.A., 1994. Shallow marine sedimentary facies in the earliest Triassic (Griesbachian) Cordilleran miogeocline, USA. Sedimentary Geology 93, 181–191.

Payne, J.L., Lehrmann, D.J., Jiayong, Wei, Orchard, M.J., Schrag, D.P., Knoll, A.H., 2004. Large perturbations of the carbon cycle during recovery from the end-Permian extinction. Science 305, 506–509.

Perri, M.C., 1991. Conodont biostratigraphy of the Werfen Formation (Lower Triassic), Southern Alps, Italy. Bolletino della Societa Paleontologica Italiana 30, 23–46.

Perri, M.C., Andraghetti, M., 1987. Permian-Triassic boundary and early Triassic conodonts from the Southern Alps, Italy. Rivista Italiana di Paleontologia e Stratigrafia 93, 291–328.

Picard, M.D., 1964. Pelwomagnetic correlation of units within Chugwater (Triassic) Formation, west-central Wyoming. Bulletin of the American Association of Petroleum Geologists 48, 269–291.

Shive, P.N., Steiner, M.B., Huycke, D.T., 1984. Magnetostratigraphy, paleomagnetism and remanence acquisition in the Triassic Chugwater Group of Wyoming. Journal of Geophysical Research 89, 1801–1815.

Shoemaker, E.M., Newman, W.L., 1959. Moenkopi Formation (Triassic? And Triassic) in Salt Anticline Region, Colorado and Utah. Bulletin of the American Association of Petroleum Geologists 43, 1835–1851.

Steiner, M.B., Morales, M., Shoemaker, E.M., 1993. Magnetostratigraphic, biostratigraphic, and lithologic correlations in the Triassic strata of the western United States. Applications of Paleomagnetism to Sedimentary Geology. SEPM, Special Publication 49, pp. 41–57.

Stephenson, M.H., Osterloff, P.L., Filatoff, J., 2003. Palynological biozonation of the Permian of Oman and Saudia Arabia: progress and challenges. GeoArabia 8, 467–496.

Stewart, J.H., Poole, F.G., Wilson, R.F., 1972. Stratigraphy and origin of the Triassic Moenkopi Formation and related strata in the Colorado Plateau region. U.S. Geological Survey Professional Paper 691.

Szurlies, M., Bachmann, G.H., Menning, M., Nowaczyk, N.R., Käding, K.C., 2003. Magnetostratigraphy and high-resolution lithostratigraphy of the Permian-Triassic boundary interval in Central Germany. Earth and Planetary Science Letters 212, 263–278.

Wignall, P.B., Hallam, A., 1992. Anoxia as a cause of the Permian/Triassic extinction: facies evidence from northern Italy and the western United States. Palaeogeography, Palaeoclimatology, Palaeoecology 93, 21–46.

Wignall, P.B., Hallam, A., 1993. Griesbachian (Earliest Triassic) palaeoenvironmental changes in the Salt Range, Pakistan and southeast China and their bearing on the Permo-Triassic mass extinction. Palaeogeography, Palaeoclimatology, Palaeoecology 102, 215–237.

Wignall, P.B., Twitchett, R.J., 2002. Permian–Triassic sedimentology of Jameson Land, East Greenland: incised submarine channels in an anoxic basin. Journal of the Geological Society 159, 691–703.

Wignall, P.B., Newton, R.J., 2003. Contrasting Deep-water Records from the Upper Permian and Lower Triassic of South Tibet and British Columbia: Evidence for a Diachronous Mass Extinction. Palaios 18, 153–167.

Wignall, P.B., Kozur, H., Hallam, A., 1996. On the timing of palaeoenvironmental changes at the Permo-Triassic (P/Tr) boundary using conodont biostratigraphy. Historical Biology 12, 39–62.

Wilgus, C.K., 1981. A stable isotope study of Permian and Triassic marine evaporite and carbonate rocks, western interior USA. PhD thesis, University of Oregon, Eugene, unpublished.

Worden, R.H., Smalley, P.C., Fallick, A.E., 1997. Sulfur cycle in buried evaporites. Geology 25, 643–646.

Yin, H., Tong, J., 1998. Multidisciplinary high-resolution correlation of the Permian-Triassic boundary. Palaeogeography, Palaeoclimatology, Palaeoecology 143, 199–212.

Yin, H., Zhang, K., Tong, J., Yang, Z., Wu, S., 2001. The Global Stratotype Section and Point (GSSP) of the Permian-Triassic boundary. Episodes 24, 102–114.

Zhu, Yanming, Liu, Yuyan, 1999. Magnetostratigraphy of the Permo-Triassic boundary section at Meishan, Changxing, Zhejiang Province. In: Yin, Hongfu, Tong, Jinnan (Eds.), Pangea and the Paleozoic-Mesozoic transition. China University of Geosciences Press, Wuhan, pp. 79–84.